

Electronic Supplementary Information

Why alloying with noble metals does not decrease the oxidation of platinum – a DFT-based ab-initio thermodynamics study

Alexander Kafka and Franziska Hess*

*Technische Universität Berlin,
Straße des 17. Juni 124, 10623 Berlin, Germany*

Table of contents:

Tab. S1	Structure and thermodynamic properties of all investigated phases compared to literature values.	2
Tab. S2	Fit parameters obtained for the vibrational heat capacity, -enthalpy and -entropy of all crystalline phases.	4
Tab. S3	Comparison of several dispersion correction methods available in VASP for the Pt(II)-oxides.	5
Fig. S1	Energy and Gibbs free energy of mixing, Gibbs free energies of platinum- and silver oxidation, as well as Gibbs free energies of electrochemical platinum- and silver oxidation of Pt–Ag.	6
Fig. S2	Energy and Gibbs free energy of mixing, Gibbs free energies of platinum- and gold oxidation, as well as Gibbs free energies of electrochemical platinum- and gold oxidation of Pt–Au.	7
Fig. S3	Energy and Gibbs free energy of mixing, Gibbs free energies of platinum- and cobalt oxidation, as well as Gibbs free energies of electrochemical platinum- and cobalt oxidation of Pt–Co.	8
Fig. S4	Energy and Gibbs free energy of mixing, Gibbs free energies of platinum- and copper oxidation, as well as Gibbs free energies of electrochemical platinum- and copper oxidation of Pt–Cu.	9
Fig. S5	Energy and Gibbs free energy of mixing, Gibbs free energies of platinum- and iridium oxidation, as well as Gibbs free energies of electrochemical platinum- and iridium oxidation of Pt–Ir.	10
Fig. S6	Energy and Gibbs free energy of mixing, Gibbs free energies of platinum- and nickel oxidation, as well as Gibbs free energies of electrochemical platinum- and nickel oxidation of Pt–Ni.	11
Fig. S7	Energy and Gibbs free energy of mixing, Gibbs free energies of platinum- and rhenium oxidation, as well as Gibbs free energies of electrochemical platinum- and rhenium oxidation of Pt–Re.	12
Fig. S8	Energy and Gibbs free energy of mixing, Gibbs free energies of platinum- and rhodium oxidation, as well as Gibbs free energies of electrochemical platinum- and rhodium oxidation of Pt–Rh.	13
Fig. S9	Energy and Gibbs free energy of mixing, Gibbs free energies of platinum- and tungsten oxidation, as well as Gibbs free energies of electrochemical platinum- and tungsten oxidation of Pt–W.	14
Fig. S10	Comparison of mean- and individual empirical enthalpy correction of the Gibbs free energies of copper- and rhodium oxidation from within Pt–Cu and Pt–Rh.	15

Tab. S1: Structure, energy of formation (ΔE_f), emp. corrected standard enthalpy of formation ($\Delta H_f^0 - n_M \cdot 38.27 \text{ kJ/mol}$) and standard entropy (S^0) of all crystalline and gaseous phases compared to selected literature values.

Phase	Structure	ΔE_f [kJ/mol]	ΔH_f^0 [kJ/mol]	$\Delta H_f^0(\text{Lit.})$ [kJ/mol]	S^0 [J/(mol·K)]	$S^0(\text{Lit.})$ [J/(mol·K)]
O ₂	<i>D_{∞h}</i>	0.00	0.00	---	205.43	205.15 ¹
H ₂	<i>D_{∞h}</i>	0.00	0.00	---	130.37	130.68 ¹
H ₂ O	<i>C_{2v}</i>	-121.72	-111.17	-121.92 ¹	94.47	94.42 ¹
Ag	<i>Fm$\bar{3}m$</i>	0.00	0.00	---	44.17	42.48 ²
Ag ₂ O	<i>Pn$\bar{3}m$</i>	-5.91	-43.39	-15.34 ³	62.51	60.95 ³
Au	<i>Fm$\bar{3}m$</i>	0.00	0.00	---	51.20	47.35 ⁴ , 47.29 ⁵
Au ₂ O ₃	<i>Fdd2</i>	-19.80	-55.16	---	56.86	---
α -Co	<i>P6₃/mmc</i>	0.00	0.00	---	27.47	30.04 ⁶ , 30.03 ⁷
β -Co	<i>Fm$\bar{3}m$</i>	1.44	1.33	---	29.43	30.66 ⁶
CoO	<i>P2/m</i> ^{a.)}	-126.51	-164.99	-236.86 ⁸ , -237.39 ⁷	48.68	54.31 ⁸ , 53.33 ⁷
Co ₃ O ₄	<i>I4₁/amd</i> ^{a.)}	-233.78	-268.87	-305.13 ⁸	35.72	36.47 ⁸
Pt ₃ Co	<i>Pm$\bar{3}m$</i>	-5.09	-5.12	---	51.06	---
PtCo	<i>P4/mmm</i>	-7.44	-7.50	---	71.24	---
Cu	<i>Fm$\bar{3}m$</i>	0.00	0.00	---	33.81	33.13 ⁹ , 33.18 ⁷
Cu ₂ O	<i>Pn$\bar{3}m$</i>	-46.42	-83.45	-85.13 ¹⁰ , -85.12 ⁷	49.53	46.34 ¹⁰ , 46.18 ⁷
CuO	<i>C2/c</i>	-108.38	-145.32	-155.19 ¹⁰	45.42	43.06 ¹⁰
Pt ₃ Cu	<i>Cmmm</i>	-10.83	-10.83	---	52.46	---
PtCu	<i>R$\bar{3}m$</i>	-14.41	-14.41	---	75.09	---
Ir	<i>Fm$\bar{3}m$</i>	0.00	0.00	---	36.43	35.49 ¹¹
IrO ₂	<i>P4₂/mnm</i>	-230.45	-263.05	-249.50 ¹² , -249.37 ¹³	49.07	51.01 ¹³
IrO ₂	<i>C_{2v}</i>	192.16	190.66	188.20 ¹⁴	286.07	274.11 ¹⁴
IrO ₃	<i>C_{2v}</i>	-9.88	-10.14	~ 22.00 ^{15 b.)}	330.23	303.20 ^{15 b.)}
Ni	<i>Fm$\bar{3}m$</i>	0.00	0.00	---	27.72	29.86 ¹⁶ , 29.87 ⁷
NiO	<i>P2/m</i> ^{a.)}	-125.43	-163.34	-239.84 ¹⁷	44.20	37.99 ⁷
Pt ₃ Ni	<i>Pm$\bar{3}m$</i>	-5.90	-5.93	---	51.46	---
PtNi	<i>P4/mmm</i>	-8.68	-8.73	---	71.23	---
Pt	<i>Fm$\bar{3}m$</i>	0.00	0.00	---	42.07	41.53 ¹⁸
PtO	<i>P4₂/mmc</i>	-42.80	-78.49	-88.50 ¹⁹	45.87	---
Pt ₃ O ₄	<i>Pm$\bar{3}n$</i>	-98.03	-133.09	-121.11 ¹⁹	54.55	---
PtO ₂	<i>P$\bar{3}m1$</i>	-134.26	-167.61	---	51.33	---
PtO ₂	<i>Pnnm</i>	-147.67	-180.89	-191.00 ¹⁹	50.43	---
PtO ₂	<i>C_{2v}</i>	160.69	160.57	218.00 ²⁰ , ~ 164.00 ²¹⁻²³	259.89	~ 250.00 ²¹⁻²³
Re	<i>P6₃/mmc</i>	0.00	0.00	---	38.27	36.48 ²⁴
ReO ₂	<i>P2₁/c</i>	-399.67	-433.09	---	50.52	---
ReO ₂	<i>Pbcn</i>	-423.79	-456.67	-445.15 ²⁵ , -444.30 ²⁶ , -448.94 ²⁷	47.75	47.83 ²⁵ , 47.82 ²⁷
ReO ₃	<i>Pm$\bar{3}m$</i>	-608.26	-640.03	-601.90 ²⁸ , -589.11 ²⁷	67.97	69.25 ²⁷
Re ₂ O ₇	<i>P2₁2₁2₁</i>	-637.68	-667.39	-631.58 ²⁷	104.20	103.64 ²⁷
Re ₂ O ₇	<i>C_{2v}</i>	-572.58	-567.95	-566.30 ²⁸	235.01	219.35 ²⁸
Rh	<i>Fm$\bar{3}m$</i>	0.00	0.00	---	32.01	31.56 ¹¹
Rh ₂ O ₃	<i>Pbca</i>	-173.12	-207.77	-202.77 ²⁹ , -202.98 ³⁰	39.63	37.85 ²⁹ , 35.75 ³⁰
Rh ₂ O ₃	<i>R$\bar{3}c$</i>	-170.66	-205.34	---	39.67	---
RhO ₂	<i>P4₂/mnm</i>	-243.29	-276.41	-244.94 ³¹	46.05	45.11 ³¹
RhO ₂	<i>C_{2v}</i>	174.61	173.23	188.87 ^{21,22} , 200.13 ²³	255.32	257.30 ^{21,22} , 264.40 ²³

a.) The *Fd $\bar{3}m$* - and *Fm $\bar{3}m$* -structures of Co₃O₄ and CoO / NiO are distorted due to their magnetic structure.

b.) and references therein

Tab. S1: Structure, energy of formation (ΔE_f), emp. corrected standard enthalpy of formation ($\Delta H_f^0 - n_M \cdot 38.27 \text{ kJ/mol}$) and standard entropy (S^0) of all crystalline and gaseous phases compared to selected literature values.(continued)

Phase	Structure	ΔE_f [kJ/mol]	ΔH_f^0 [kJ/mol]	$\Delta H_f^0(\text{Lit.})$ [kJ/mol]	S^0 [J/(mol·K)]	$S^0(\text{Lit.})$ [J/(mol·K)]
W	$I\bar{m}\bar{3}m$	0.00	0.00	---	34.04	32.66 ³²
WO ₂	$P2_1/c$	-562.31	-596.16	-586.55 ³³ , -589.69 ¹	50.84	50.53 ¹
WO ₂	C_{2v}	25.24	24.78	~76.57 ¹	273.53	285.50 ¹
W ₁₈ O ₄₉	$P2/m$	-759.66	-792.31	-779.70 ³³ , -781.15 ¹	67.21	68.43 ¹
WO ₃	$P2_1/c$	-822.09	-853.90	---	78.45	---
WO ₃	$Pnma$	-821.66	-853.34	-842.91 ^{1,33}	80.15	76.57 ³⁴ , 75.91 ¹
WO ₃	$P4/ncc$	-820.59	-853.29	---	78.98	---
WO ₃	C_{3v}	-326.08	-325.04	~ -292.88 ¹	290.70	286.44 ¹
Pt ₂ W	$Imm\bar{m}$	-34.46	-34.47	---	56.85	---
PtW	$P\bar{6}m2$	-10.70	-10.73	---	77.26	---

- a.) The $Fd\bar{3}m$ - and $Fm\bar{3}m$ -structures of Co₃O₄ and CoO / NiO are distorted due to their magnetic structure.
b.) and references therein

- 1 M. W. J. Chase, *NIST-JANAF Thermochemical Tables*, American Institute of Physics, 4th edn., 1998.
- 2 J. W. Arblaster, *J. Phase Equil. Diffus.*, 2015, **36**, 573–591.
- 3 J. Assal, B. Hallstedt and L. J. Gauckler, *J. Am. Ceram. Soc.*, 1997, **80**, 3054–3060.
- 4 A. V. Khvan, I. A. Uspenskaya, N. M. Aristova, Q. Chen, G. Trimarchi, N. M. Konstantinova and A. T. Dinsdale, *Calphad*, 2020, **68**, 101724.
- 5 J. W. Arblaster, *J. Phase Equil. Diffus.*, 2016, **37**, 229–245.
- 6 A. Fernández Guillermet, *Int. J. Thermophys.*, 1987, **8**, 481–510.
- 7 R. D. Holmes, H. S. C. O'Neill and R. J. Arculus, *Geochim. Cosmochim. Acta*, 1986, **50**, 2439–2452.
- 8 M. Chen, B. Hallstedt and L. J. Gauckler, *J. Phase Equilibria*, 2003, **24**, 212–227.
- 9 J. W. Arblaster, *J. Phase Equil. Diffus.*, 2015, **36**, 422–444.
- 10 B. Hallstedt, D. Risold and L. J. Gauckler, *J. Phase Equilibria*, 1994, **15**, 483–499.
- 11 J. W. Arblaster, *Platin. Met. Rev.*, 1996, **40**, 62–63.
- 12 H. S. C. O'Neill and J. Nell, *Geochim. Cosmochim. Acta*, 1997, **61**, 5279–5293.
- 13 E. H. P. Cordfunke, *Thermochim. Acta*, 1981, **50**, 177–185.
- 14 R. T. Wimber, S. W. Hills, N. K. Wahl and C. R. Tempero, *Metall. Trans. A*, 1977, **8**, 193–199.
- 15 J. H. Carpenter, *J. Less-Common Met.*, 1989, **152**, 35–45.
- 16 P. D. Desai, *Int. J. Thermophys.*, 1987, **8**, 763–780.
- 17 H. S. C. O'Neill and M. I. Pownceby, *Contrib. Mineral. Petrol.*, 1993, **114**, 296–314.
- 18 J. W. Arblaster, *Platin. Met. Rev.*, 2005, **49**, 141–149.
- 19 C.-B. Wang, H.-K. Lin, S.-N. Hsu, T.-H. Huang and H.-C. Chiu, *J. Mol. Catal. A: Chem.*, 2002, **188**, 201–208.
- 20 M. Citir, R. B. Metz, L. Belau and M. Ahmed, *J. Phys. Chem. A*, 2008, **112**, 9584–9590.
- 21 C. B. Alcock and G. W. Hooper, *Proc. R. Soc. London, Ser. A.*, 1960, **254**, 551–561.
- 22 C. B. Alcock, *Platin. Met. Rev.*, 1961, **5**, 134–139.
- 23 A. Olivei, *J. Less-Common Met.*, 1972, **29**, 11–23.
- 24 J. W. Arblaster, *Calphad*, 1996, **20**, 343–352.
- 25 K. T. Jacob, S. Mishra and Y. Waseda, *Thermochim. Acta*, 2000, **348**, 61–68.
- 26 M. I. Pownceby and H. S. C. O'Neill, *Contrib. Mineral. Petrol.*, 1994, **118**, 130–137.
- 27 J. M. Stuve and M. J. Ferrante, *Thermodynamic properties of rhenium oxides, 8 to 1,400 K*, Dept. of the Interior, Bureau of Mines, Washington, D.C., 1976.
- 28 H. Oppermann, *Z. Anorg. Allg. Chem.*, 1985, **523**, 135–144.
- 29 K. T. Jacob, T. Uda, T. H. Okabe and Y. Waseda, *High. Temp. Mat. Pr.-ISR*, 2000, **19**, 11–16.
- 30 J. Nell and H. S. C. O'Neill, *Geochim. Cosmochim. Acta*, 1997, **61**, 4159–4171.
- 31 K. T. Jacob and D. Prusty, *J. Alloys Compd.*, 2010, **507**, L17–L20.
- 32 J. W. Arblaster, *J. Phase Equil. Diffus.*, 2018, **39**, 891–907.
- 33 T. V. Charlu and O. J. Kleppa, *J. Chem. Thermodyn.*, 1973, **5**, 325–330.
- 34 B.-y. Han, A. V. Khoroshilov, A. V. Tyurin, A. E. Baranchikov, M. I. Razumov, O. S. Ivanova, K. S. Gavrichev and V. K. Ivanov, *J. Therm. Anal. Calorim.*, 2020, **142**, 1533–1543.

Tab. S2: Fit parameters obtained for the vibrational heat capacity $C_{vib}(T)$, enthalpy $H_{vib}(T)$ and entropy $S_{vib}(T)$ of all crystalline phases between 300 K and 1300 K per formula unit. The corrected single-point energy E_{corr} already contains the mean empirical correction of 38.27 kJ/mol per metal atom. Please see below, how the parameters are related.

Phase	Structure	E_{corr} [kJ/mol]	a_1 [J/(mol·K)]	a_2 [J/(mol·K ²)]	a_3 [J/(mol·K ³)]	a_4 [J/(mol·K ⁴)]	a_5 [J-K/mol]	a_6 [J/mol]	a_7 [J/(mol·K)]
Ag	<i>Fm</i> ³ <i>m</i>	-318.27	2.336E+01	4.863E-03	-5.140E-06	1.799E-09	9.966E-01	4.616E+02	-9.016E+01
Ag ₂ O	<i>Pn</i> ³ <i>m</i>	-1200.57	5.028E+01	7.168E-02	-7.345E-05	2.519E-08	9.597E-01	7.883E+03	-1.798E+02
Au	<i>Fm</i> ³ <i>m</i>	-373.10	2.396E+01	3.038E-03	-3.214E-06	1.125E-09	9.978E-01	2.875E+02	-8.606E+01
Au ₂ O ₃	<i>Fdd</i> 2	-2289.35	5.226E+01	2.088E-01	-2.123E-04	7.246E-08	9.989E-01	2.381E+04	-2.375E+02
α -Co	<i>P</i> 6 ₃ /mmc	-719.52	1.921E+01	1.747E-02	-1.836E-05	6.400E-09	9.881E-01	1.705E+03	-8.640E+01
β -Co	<i>Fm</i> ³ <i>m</i>	-718.08	2.015E+01	1.463E-02	-1.540E-05	5.375E-09	9.899E-01	1.417E+03	-8.910E+01
CoO	<i>P</i> 2/ <i>m</i>	-1359.96	3.049E+01	5.367E-02	-5.584E-05	1.935E-08	9.661E-01	5.498E+03	-1.388E+02
Co ₃ O ₄	<i>I</i> 4 ₁ /amd	-4877.38	5.069E+01	3.589E-01	-3.660E-04	1.252E-07	9.981E-01	4.035E+04	-2.735E+02
Pt ₃ Co	<i>Pm</i> ³ <i>m</i>	-2726.33	8.933E+01	3.201E-02	-3.378E-05	1.181E-08	9.776E-01	3.061E+03	-3.640E+02
PtCo	<i>P</i> 4/mmm	-1396.55	4.328E+01	2.022E-02	-2.131E-05	7.444E-09	9.860E-01	1.945E+03	-1.805E+02
Cu	<i>Fm</i> ³ <i>m</i>	-416.84	2.134E+01	1.101E-02	-1.161E-05	4.054E-09	9.924E-01	1.060E+03	-9.060E+01
Cu ₂ O	<i>Pn</i> ³ <i>m</i>	-1478.72	4.254E+01	9.222E-02	-9.324E-05	3.170E-08	9.995E-01	1.077E+04	-1.670E+02
CuO	<i>C</i> 2/ <i>c</i>	-1039.15	2.610E+01	6.996E-02	-7.208E-05	2.481E-08	9.590E-01	7.513E+03	-1.212E+02
Pt ₃ Cu	<i>C</i> mmm	-2446.61	9.015E+01	2.952E-02	-3.116E-05	1.089E-08	9.793E-01	2.819E+03	-3.638E+02
PtCu	<i>R</i> 3 <i>m</i>	-1107.82	4.419E+01	1.744E-02	-1.840E-05	6.429E-09	9.879E-01	1.674E+03	-1.811E+02
Ir	<i>Fm</i> ³ <i>m</i>	-923.97	2.228E+01	8.177E-03	-8.632E-06	3.019E-09	9.943E-01	7.805E+02	-9.258E+01
IrO ₂	<i>P</i> 4 ₂ /mnm	-2144.03	1.837E+01	1.580E-01	-1.577E-04	5.315E-08	9.993E-01	1.953E+04	-9.614E+01
Ni	<i>Fm</i> ³ <i>m</i>	-573.18	1.926E+01	1.729E-02	-1.817E-05	6.336E-09	9.883E-01	1.688E+03	-8.644E+01
NiO	<i>P</i> 2/ <i>m</i>	-1212.55	3.057E+01	5.796E-02	-6.040E-05	2.094E-08	9.631E-01	5.897E+03	-1.448E+02
Pt ₃ Ni	<i>Pm</i> ³ <i>m</i>	-2583.23	8.933E+01	3.201E-02	-3.378E-05	1.181E-08	9.776E-01	3.063E+03	-3.627E+02
PtNi	<i>P</i> 4/mmm	-1252.68	4.312E+01	2.068E-02	-2.180E-05	7.614E-09	9.857E-01	1.992E+03	-1.797E+02
Pt	<i>Fm</i> ³ <i>m</i>	-662.15	2.296E+01	6.085E-03	-6.426E-06	2.248E-09	9.957E-01	5.796E+02	-9.030E+01
PtO	<i>P</i> 4 ₂ /mmc	-1218.89	2.044E+01	8.445E-02	-8.560E-05	2.915E-08	9.996E-01	9.754E+03	-9.224E+01
Pt ₃ O ₄	<i>P</i> m ³ <i>n</i>	-4298.03	6.990E+01	2.884E-01	-2.872E-04	9.666E-08	9.987E-01	3.594E+04	-3.087E+02
PtO ₂	<i>P</i> 3 <i>m</i> 1	-1786.02	1.877E+01	1.611E-01	-1.635E-04	5.574E-08	9.992E-01	1.850E+04	-9.687E+01
PtO ₂	<i>P</i> nmm	-1799.44	2.036E+01	1.546E-01	-1.556E-04	5.278E-08	9.992E-01	1.839E+04	-1.052E+02
Re	<i>P</i> 6 ₃ /mmc	-1261.66	2.238E+01	7.382E-03	-7.794E-06	2.725E-09	9.948E-01	7.046E+02	-9.114E+01
ReO ₂	<i>P</i> 2 ₁ / <i>c</i>	-2650.94	2.253E+01	1.479E-01	-1.487E-04	5.038E-08	9.993E-01	1.777E+04	-1.158E+02
ReO ₂	<i>P</i> bcn	-2675.06	1.948E+01	1.560E-01	-1.564E-04	5.289E-08	9.992E-01	1.892E+04	-1.033E+02
ReO ₃	<i>Pm</i> ³ <i>m</i>	-3335.20	2.926E+01	1.963E-01	-1.959E-04	6.608E-08	9.991E-01	2.433E+04	-1.491E+02
Re ₂ O ₇	<i>P</i> 2 ₁ 2 ₁ 2 ₁	-7204.91	7.786E+01	3.644E-01	-3.438E-04	1.117E-07	9.989E-01	5.656E+04	-3.295E+02
Rh	<i>Fm</i> ³ <i>m</i>	-764.58	2.110E+01	1.175E-02	-1.239E-05	4.327E-09	9.918E-01	1.130E+03	-9.122E+01
Rh ₂ O ₃	<i>P</i> bca	-3378.95	3.661E+01	2.544E-01	-2.590E-04	8.847E-08	9.986E-01	2.884E+04	-1.944E+02
Rh ₂ O ₃	<i>R</i> 3 <i>c</i>	-3374.05	3.671E+01	2.544E-01	-2.591E-04	8.851E-08	9.986E-01	2.877E+04	-1.949E+02
RhO ₂	<i>P</i> 4 ₂ /mnm	-1997.48	1.898E+01	1.580E-01	-1.588E-04	5.378E-08	9.992E-01	1.896E+04	-1.026E+02
W	<i>Im</i> ³ <i>m</i>	-1323.22	2.162E+01	1.017E-02	-1.073E-05	3.748E-09	9.929E-01	9.754E+02	-9.174E+01
WO ₂	<i>P</i> 2 ₁ / <i>c</i>	-2875.14	2.370E+01	1.453E-01	-1.465E-04	4.972E-08	9.993E-01	1.724E+04	-1.214E+02
W ₁₈ O ₄₉	<i>P</i> 2/ <i>m</i>	-61488.57	5.522E+02	3.128E+00	-3.123E-03	1.053E-06	9.852E-01	3.885E+05	-2.740E+03
WO ₃	<i>P</i> 2 ₁ / <i>c</i>	-3610.59	3.594E+01	1.713E-01	-1.674E-04	5.570E-08	9.993E-01	2.332E+04	-1.705E+02
WO ₃	<i>P</i> nma	-3610.16	3.668E+01	1.699E-01	-1.658E-04	5.511E-08	9.993E-01	2.329E+04	-1.726E+02
WO ₃	<i>P</i> 4/ncc	-3610.59	3.594E+01	1.713E-01	-1.674E-04	5.570E-08	9.993E-01	2.332E+04	-1.705E+02
Pt ₂ W	<i>Imm</i> m	-2750.89	6.727E+01	2.274E-02	-2.401E-05	8.397E-09	9.840E-01	2.170E+03	-2.753E+02
PtW	<i>P</i> 6 <i>m</i> 2	-2006.78	4.503E+01	1.491E-02	-1.574E-05	5.503E-09	9.895E-01	1.423E+03	-1.831E+02

$$G(T) = H(T) + TS(T) = E_{corr} + H_{vib}(T) - TS_{vib}(T)$$

$$C_{vib}(T) = a + bT + cT^2 + dT^3 - e/T^2$$

$$H_{vib}(T) = aT + bT^2/2 + cT^3/3 + dT^4/4 - e/T + f$$

$$S_{vib}(T) = a \ln(T) + bT + cT^2/2 + dT^3/3 - e/2T^2 + g$$

Tab. S3: Comparison of several dispersion correction methods available in VASP 5 and VASP 6 for the Pt(II)-oxides. All calculations employed the PBE functional. While the energies of formation (ΔE_f) listed here are not directly comparable to experimental data, none of the methods except PBE-D3/BJ provides a reasonable estimate for the enthalpy of formation of gaseous PtO_2 (see Tab. S1), which is critical for this investigation. At the same time, based on the c -lattice parameter PBE-D3/BJ determines the best geometries.

	O ₂	Pt	$\alpha\text{-PtO}_2$				$\beta\text{-PtO}_2$				PtO ₂ (g)		
	<i>E</i>	<i>E</i>	<i>c</i>	<i>E</i>	ΔE_f	<i>c</i>	<i>E</i>	ΔE_f	<i>c</i>	<i>E</i>	ΔE_f		
	[kJ/mol]	[kJ/mol]	[Å]	[kJ/mol]	[kJ/mol]	[Å]	[kJ/mol]	[kJ/mol]	[Å]	[kJ/mol]	[kJ/mol]		
EXP	---	---	3.92 ¹	---	---	4.16 ²	---	---	3.14 ³	---	---		
PBE	-951.34	-587.75	3.97	-1684.36	-145.28	4.63	-1685.72	-146.63	3.18	-1449.60	89.49		
MBD@rSC/FI	-951.34	-587.73	3.97	-1684.88	-145.81	4.78	-1685.93	-146.86	3.18	-1449.60	89.47		
DDsC	-951.34	-587.73	3.97	-1684.88	-145.81	4.78	-1685.93	-146.86	3.18	-1449.60	89.47		
TS/HI	-951.34	-635.78	3.93	-1727.13	-140.01	4.23	-1739.30	-152.17	3.17	-1449.97	137.16		
D3/BJ	-952.04	-661.45	3.92	-1747.75	-134.26	4.15	-1761.17	-147.67	3.17	-1453.51	159.99		
BEEF-vdW	-603.08	-296.15	3.99	-1056.97	-157.74	4.39	-1062.35	-163.13	3.19	-780.99	118.24		
vdW-DF2	-582.73	-251.95	4.11	-1039.39	-204.71	4.22	-1054.37	-219.69	3.26	-819.78	14.90		
optB86b-vdW	-605.81	-368.68	3.95	-1156.50	-182.01	4.07	-1170.74	-196.25	3.17	-842.11	132.37		

1 R. W. G. Wyckoff, *Crystal Structures*, Interscience Publishers, New York, 2nd edn., 1963, **1**, 7–83.

2 H. R. Hoekstra, S. Siegel and F. X. Gallagher, *Advances in Chemistry*, American Chemical Society, Washington, D.C., 1971, **98**, 39–53.

3 K.-J. Range, F. Rau, U. Klement, A. M. Heyns, *Mater. Res. Bull.*, 1987, **22**, 1541–1547.

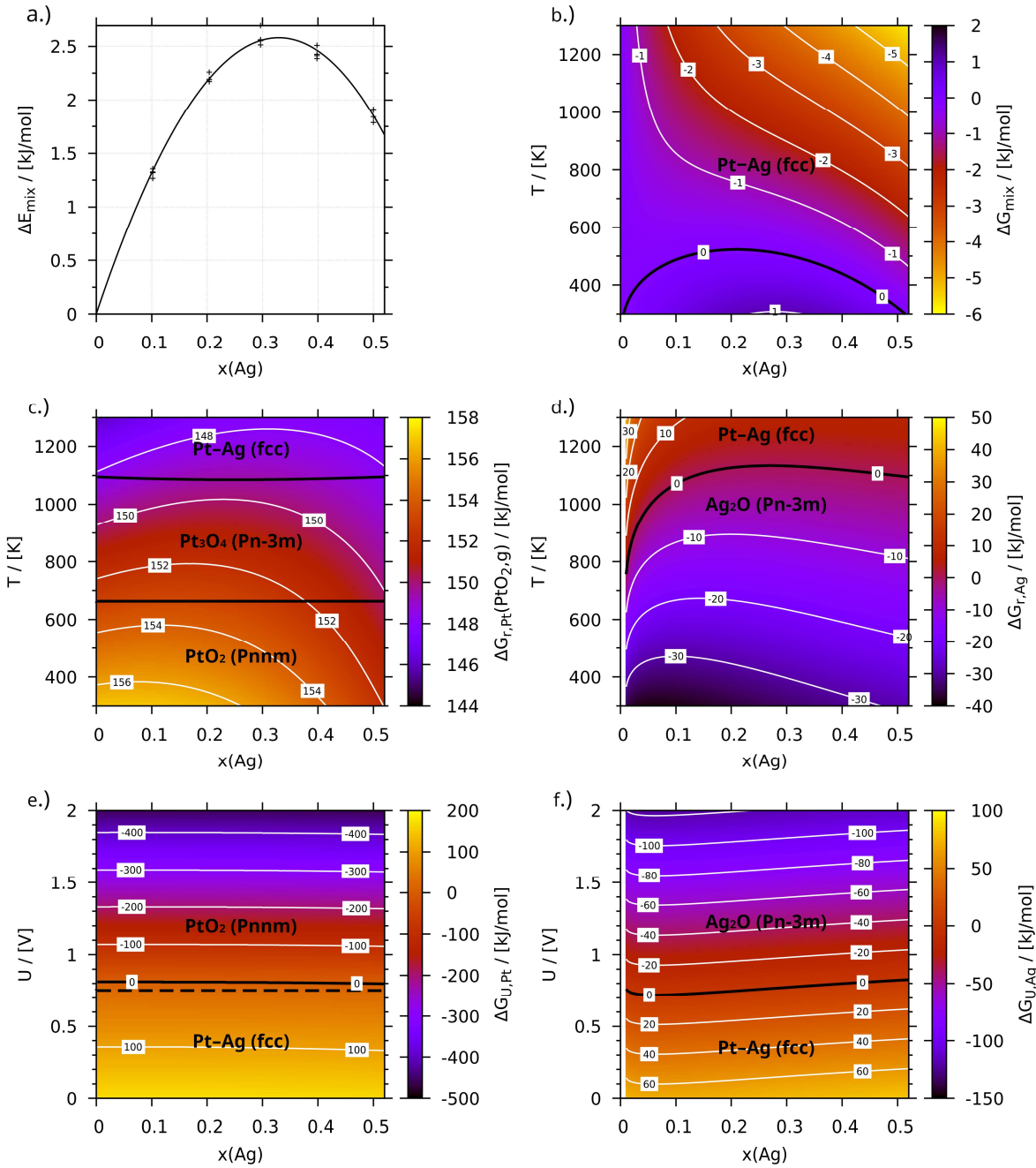


Fig. S1: Mixing energy (a), Gibbs free energy of mixing (b), Gibbs free energy of PtO_2 formation (c), Gibbs free energy of silver oxidation (d), Gibbs free energy of electrochemical platinum oxidation ($pH=0$, $T=298.15$ K) (e) and Gibbs free energy of electrochemical silver oxidation ($pH=0$, $T=298.15$ K) (f) of Pt–Ag. Phases and their boundaries are signified in black.

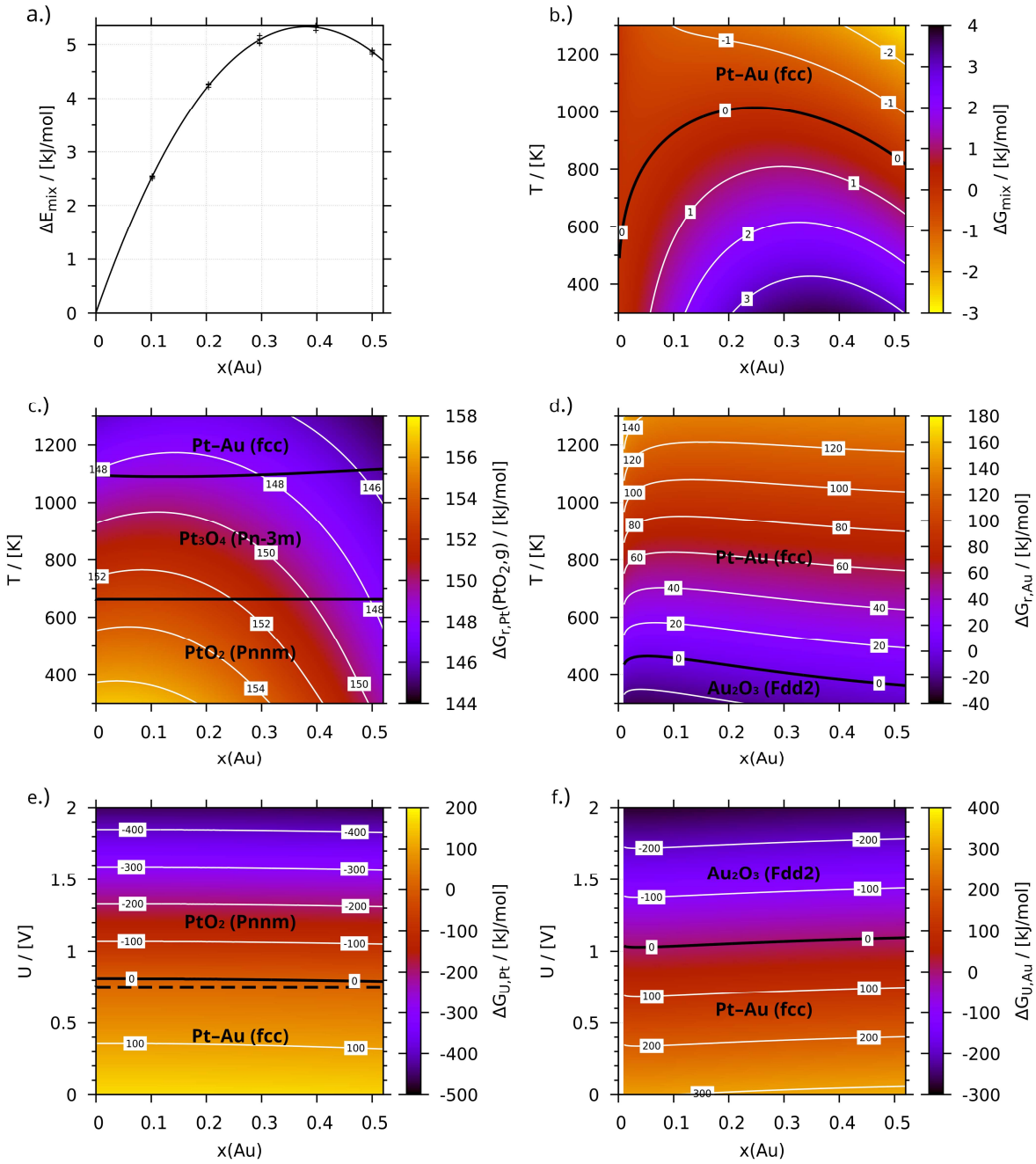


Fig. S2: Mixing energy (a), Gibbs free energy of mixing (b), Gibbs free energy of PtO_2 formation (c), Gibbs free energy of gold oxidation (d), Gibbs free energy of electrochemical platinum oxidation ($pH=0$, $T=298.15 \text{ K}$) (e) and Gibbs free energy of electrochemical gold oxidation ($pH=0$, $T=298.15 \text{ K}$) (f) of Pt–Au. Phases and their boundaries are signified in black.

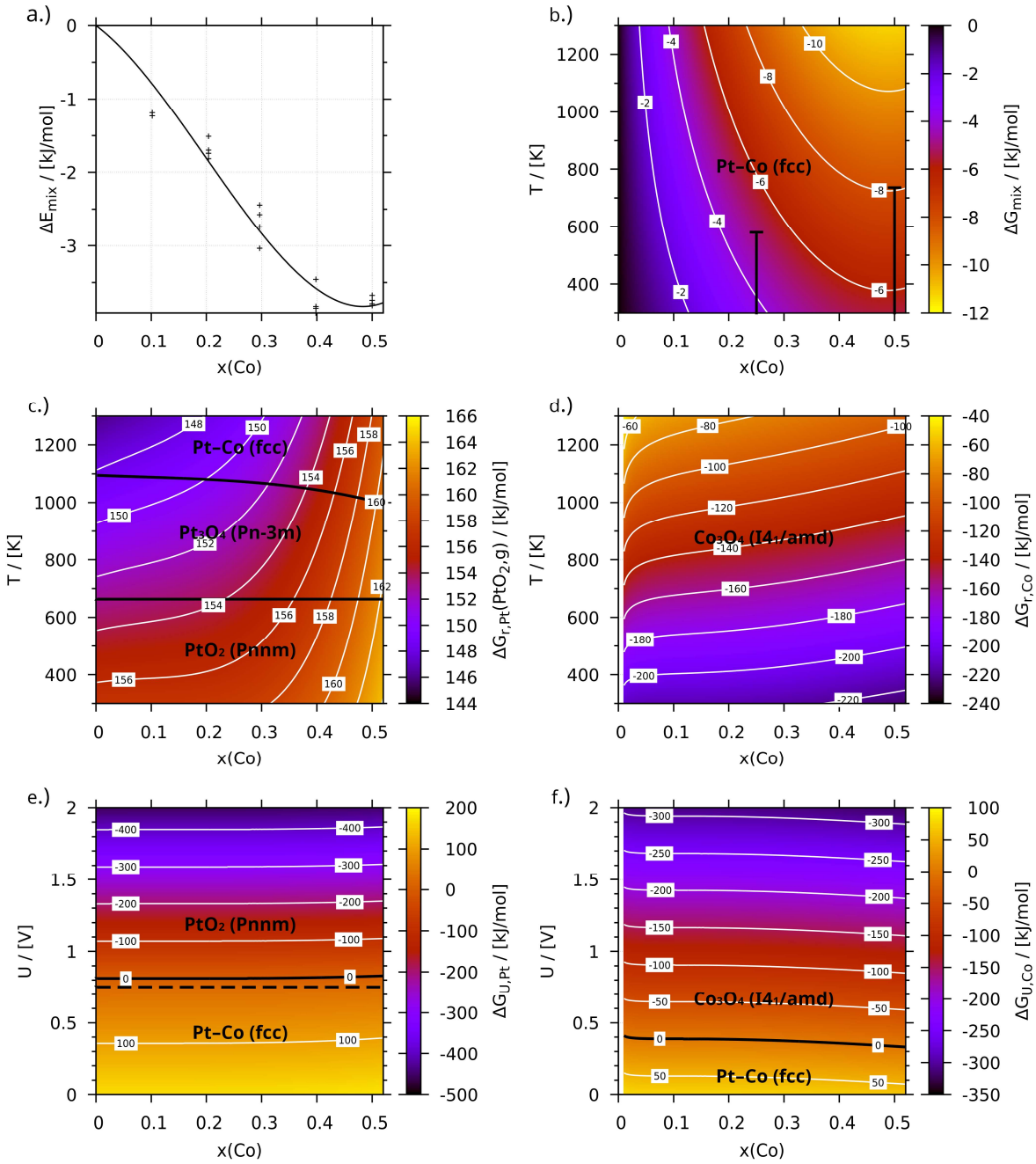


Fig. S3: Mixing energy (a), Gibbs free energy of mixing (b), Gibbs free energy of PtO_2 formation (c), Gibbs free energy of cobalt oxidation (d), Gibbs free energy of electrochemical platinum oxidation ($pH=0$, $T=298.15 \text{ K}$) (e) and Gibbs free energy of electrochemical cobalt oxidation ($pH=0$, $T=298.15 \text{ K}$) (f) of Pt–Co. Phases and their boundaries are signified in black. The $Fd\bar{3}m$ -structure of Co_3O_4 is deformed due to its magnetic structure.

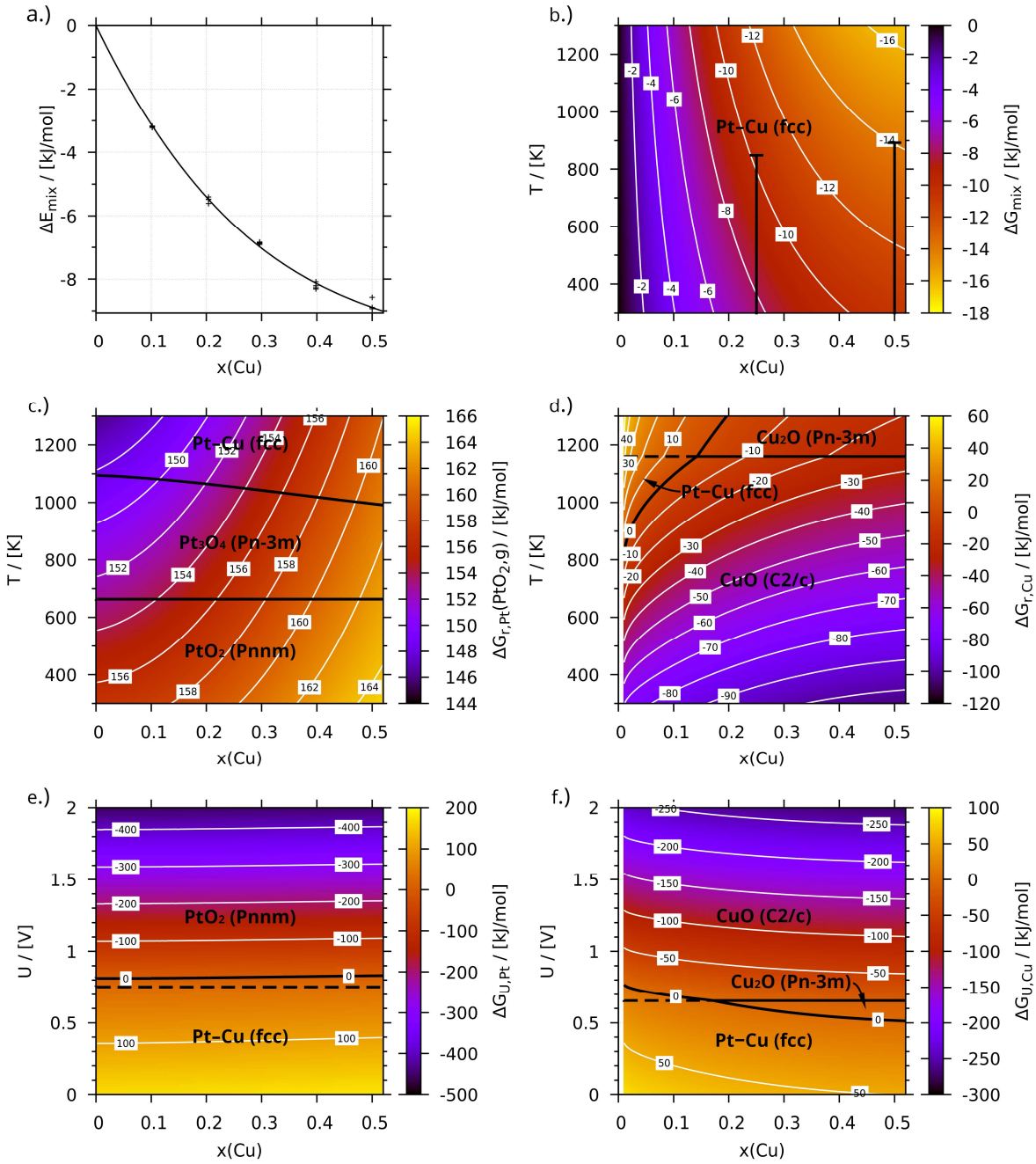


Fig. S4: Mixing energy (a), Gibbs free energy of mixing (b), Gibbs free energy of PtO_2 formation (c), Gibbs free energy of copper oxidation (d), Gibbs free energy of electrochemical platinum oxidation ($pH=0$, $T=298.15$ K) (e) and Gibbs free energy of electrochemical copper oxidation ($pH=0$, $T=298.15$ K) (f) of Pt–Cu. Phases and their boundaries are signified in black.

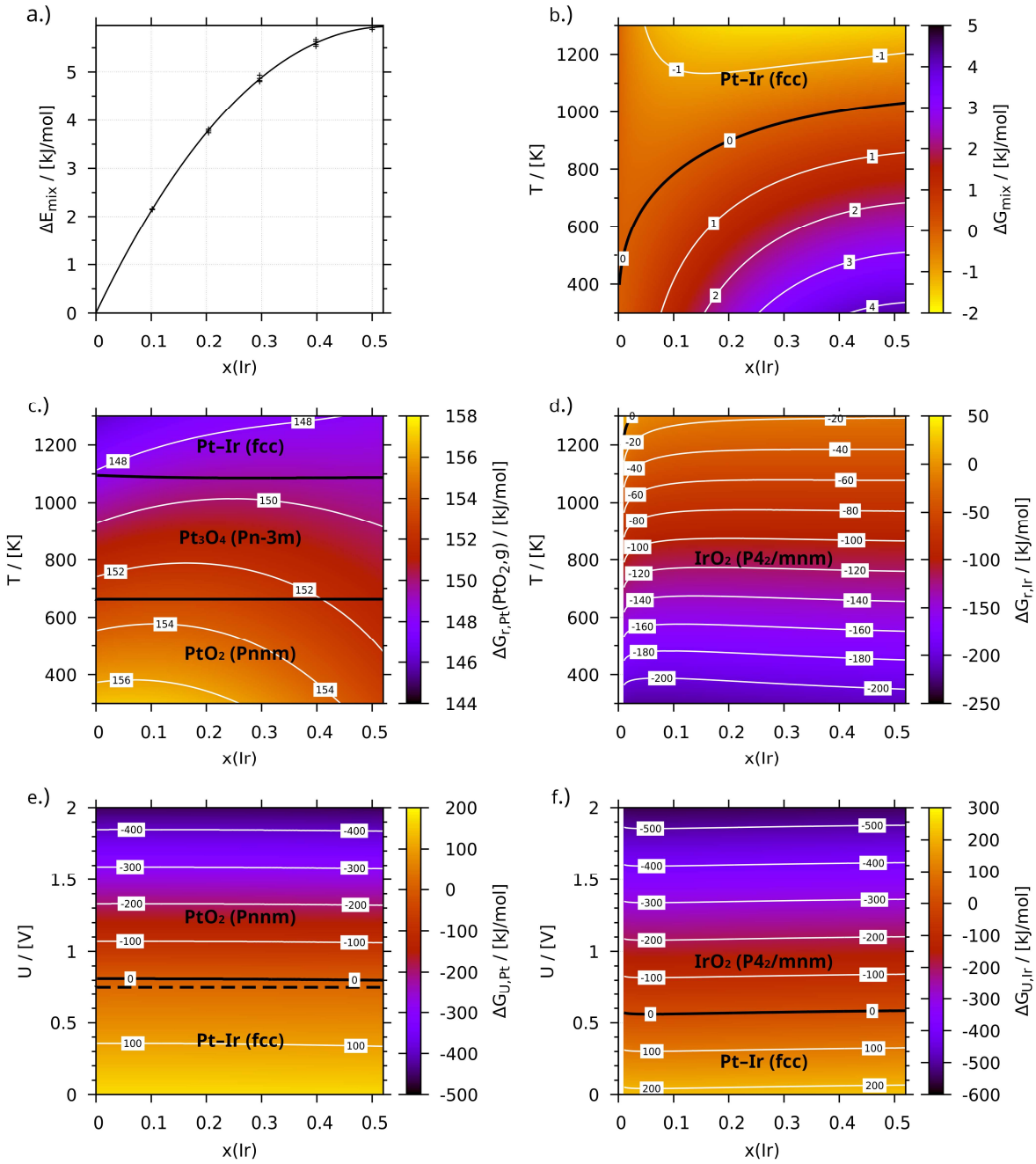


Fig. S5: Mixing energy (a), Gibbs free energy of mixing (b), Gibbs free energy of PtO_2 formation (c), Gibbs free energy of iridium oxidation (d), Gibbs free energy of electrochemical platinum oxidation ($pH=0$, $T=298.15$ K) (e) and Gibbs free energy of electrochemical iridium oxidation ($pH=0$, $T=298.15$ K) (f) of Pt–Ir. Phases and their boundaries are signified in black.

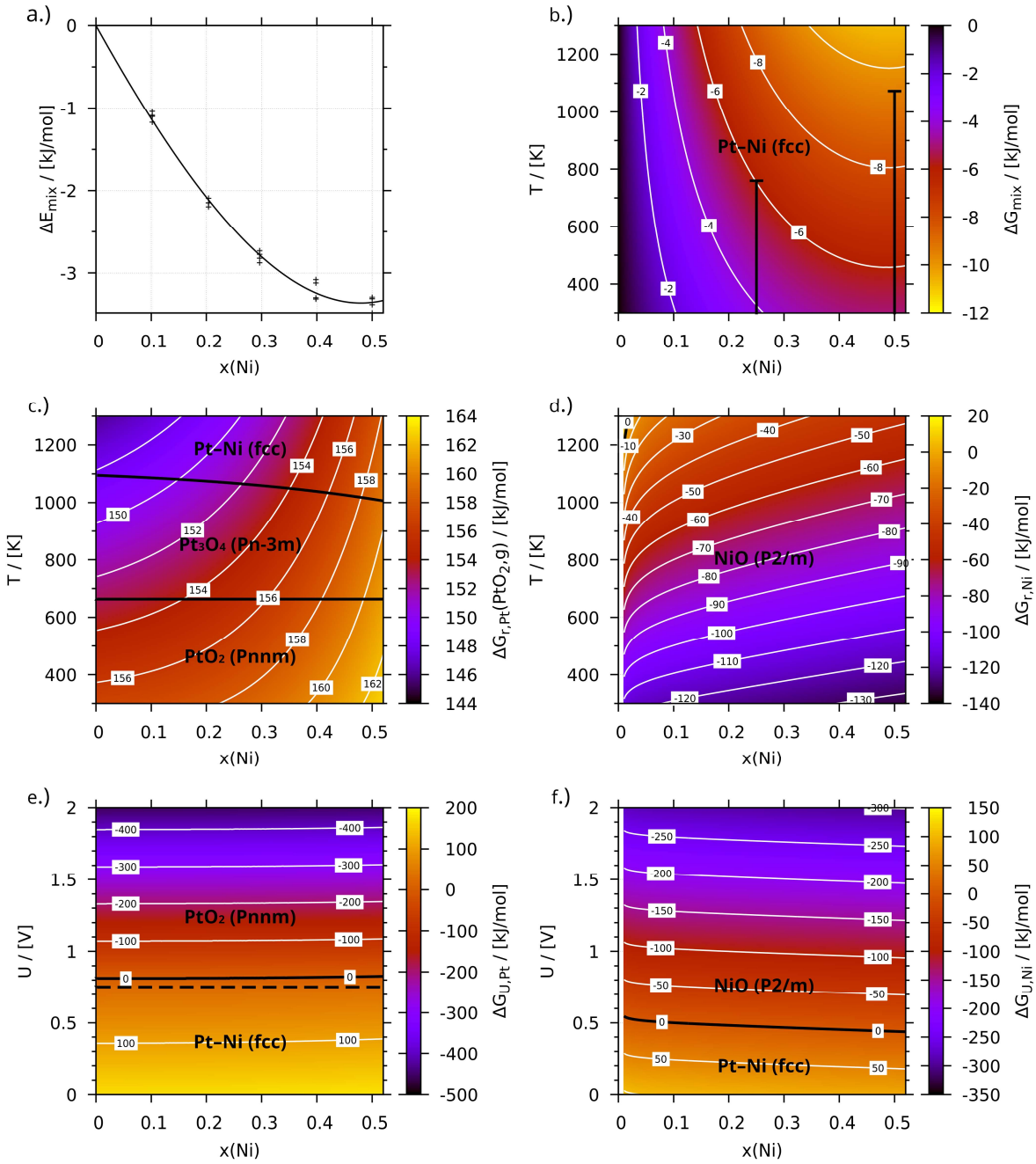


Fig. S6: Mixing energy (a), Gibbs free energy of mixing (b), Gibbs free energy of PtO_2 formation (c), Gibbs free energy of nickel oxidation (d), Gibbs free energy of electrochemical platinum oxidation ($pH=0$, $T=298.15 \text{ K}$) (e) and Gibbs free energy of electrochemical nickel oxidation ($pH=0$, $T=298.15 \text{ K}$) (f) of $\text{Pt}-\text{Ni}$. Phases and their boundaries are signified in black. The $Fm\bar{3}m$ -structure of NiO is distorted due to its magnetic structure.

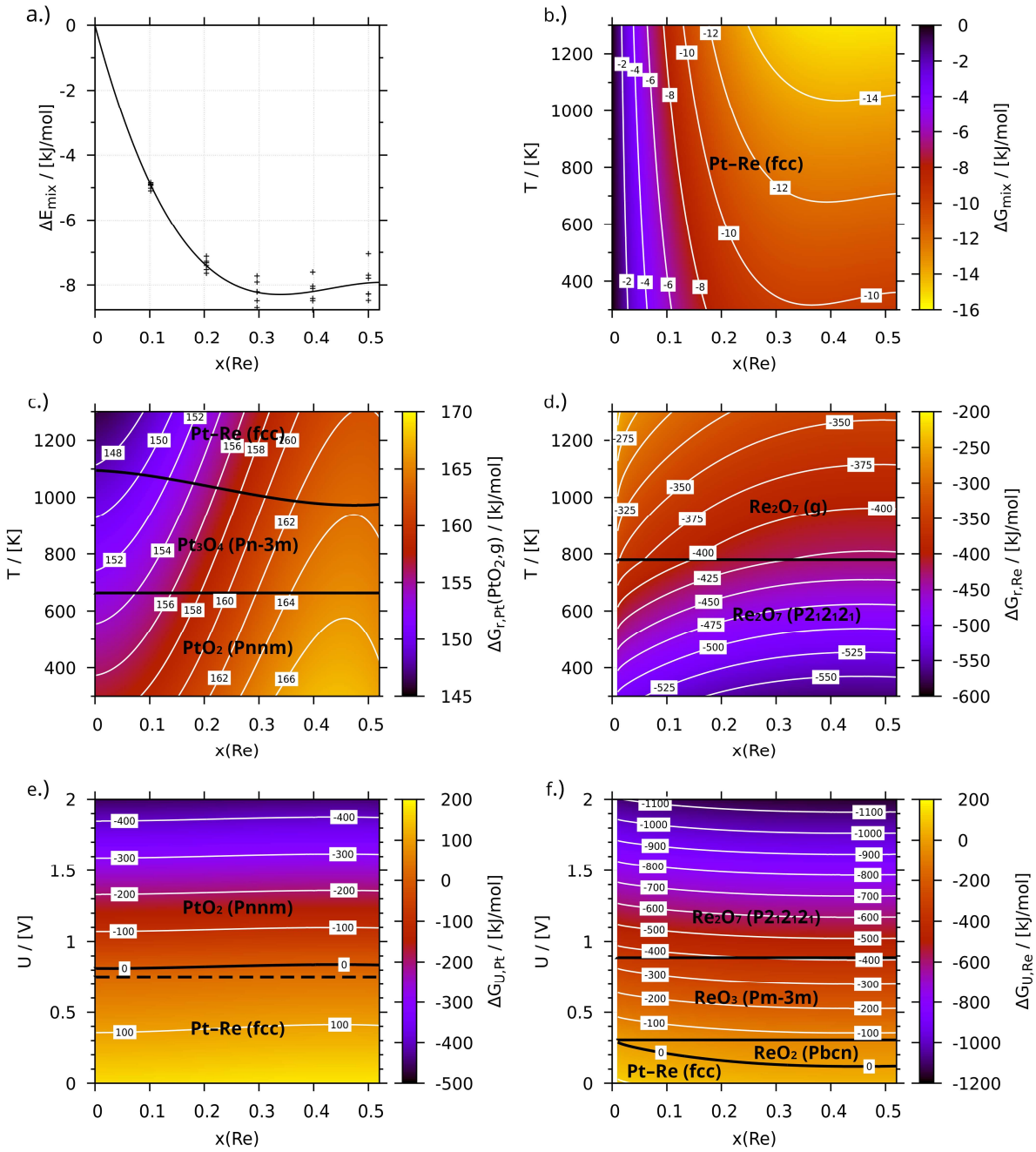


Fig. S7: Mixing energy (a), Gibbs free energy of mixing (b), Gibbs free energy of PtO_2 formation (c), Gibbs free energy of rhenium oxidation (d), Gibbs free energy of electrochemical platinum oxidation ($pH=0$, $T=298.15$ K) (e) and Gibbs free energy of electrochemical rhenium oxidation ($pH=0$, $T=298.15$ K) (f) of Pt–Re. Phases and their boundaries are signified in black.

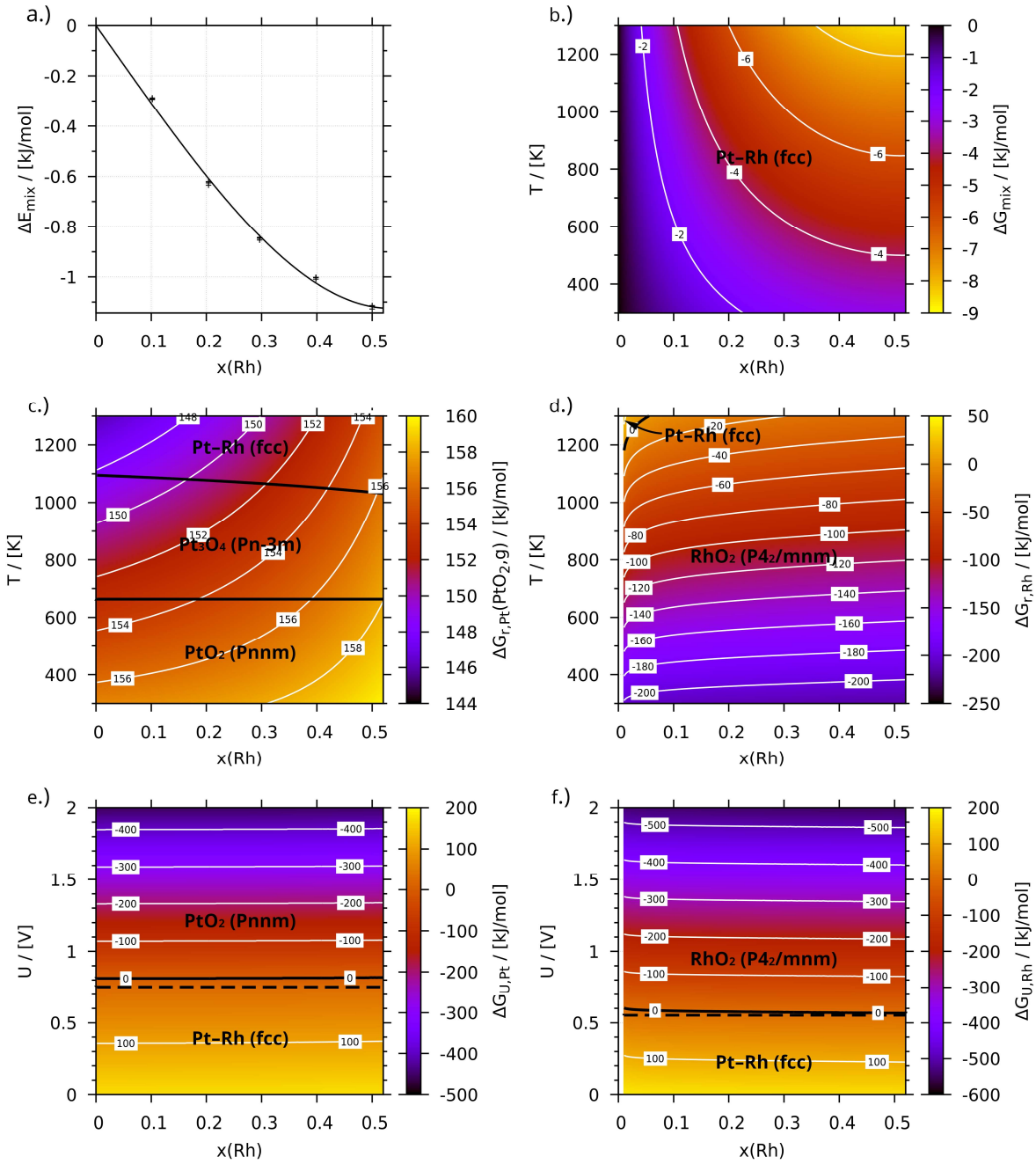


Fig. S8: Mixing energy (a), Gibbs free energy of mixing (b), Gibbs free energy of PtO_2 formation (c), Gibbs free energy of rhodium oxidation (d), Gibbs free energy of electrochemical platinum oxidation ($pH=0$, $T=298.15 \text{ K}$) (e) and Gibbs free energy of electrochemical rhodium oxidation ($pH=0$, $T=298.15 \text{ K}$) (f) of Pt–Rh. Phases and their boundaries are signified in black.

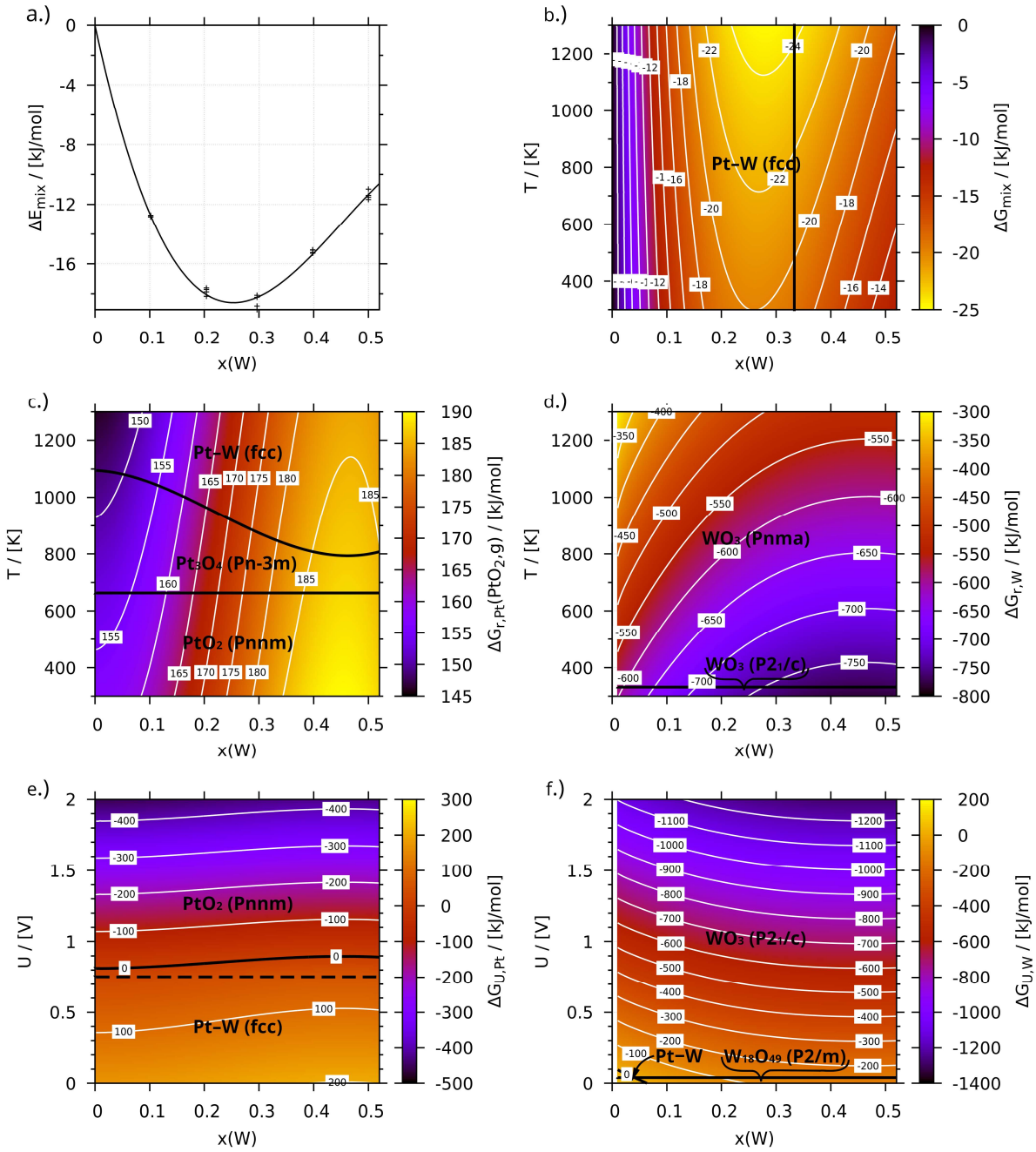


Fig. S9: Mixing energy (a), Gibbs free energy of mixing (b), Gibbs free energy of PtO_2 formation (c), Gibbs free energy of tungsten oxidation (d), Gibbs free energy of electrochemical platinum oxidation ($pH=0$, $T=298.15$ K) (e) and Gibbs free energy of electrochemical tungsten oxidation ($pH=0$, $T=298.15$ K) (f) of $\text{Pt}-\text{W}$. Phases and their boundaries are signified in black.

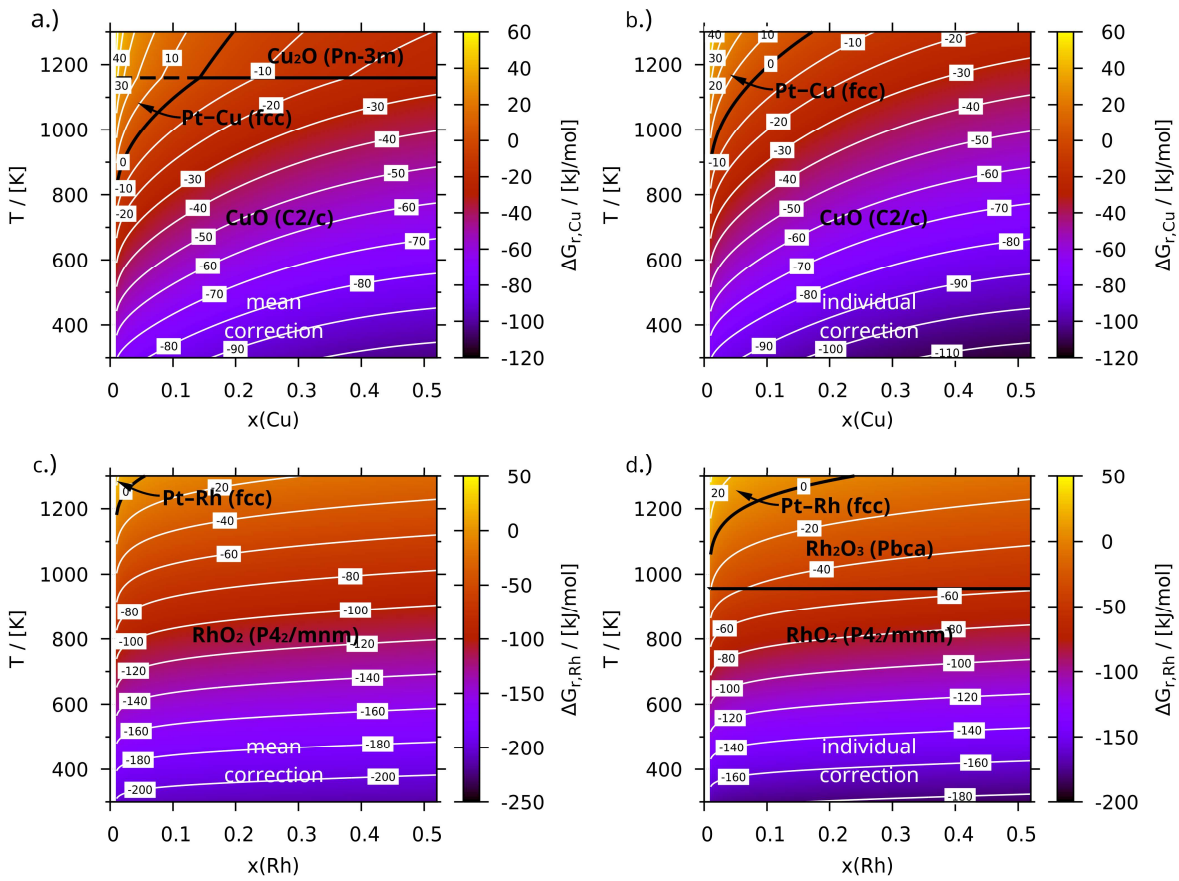


Fig. S10: Gibbs free energy of copper- (a,b) and rhodium oxidation (c,d) with mean empirical and individual correction based on the oxide enthalpies of formation. Phases and their boundaries are signified in black.